Vol 13 No 6, June 2004
1009-1963/2004/13(06)/0882-05

Chinese Physics

© 2004 Chin. Phys. Soc.
and IOP Publishing Ltd

All-optical NOT and XOR logic operation at 2.5 Gb/s based on semiconductor optical amplifier loop mirror*

Wang Ying(王 颖)†, Zhang Xin-Liang(张新亮), and Huang De-Xiu(黄德修)

Department of Optoelectronic Engineering, Huazhong University of Science and Technology, Wuhan 430074, *China*

(Received 16 October 2003; revised manuscript received 13 January 2004)

All-optical XOR and NOT logic operations based on semiconductor optical amplifier loop mirror (SLALOM) are simultaneously demonstrated theoretically and experimentally. Based on a segmented semiconductor optical amplifier model, the all-optical logic operation process is simulated theoretically. In an experimental study, 2.5 Gb/s all-optical XOR operation was achieved in the output port of SLALOM, while all-optical NOT operation was achieved in the input port through a circulator at the same time.

Keywords: all-optical logic operation, semiconductor optical amplifier, semiconductor optical amplifier loop mirror
PACC: 4280V, 4265, 4260F

1. Introduction

All-optical signal processing is expected to have a wide application in the field of all-optical communication and computation due to its capability of handling a large bandwidth of signals and a great deal of information flow. The all-optical logic operation is a key function in all-optical signal processing. Various schemes for all-optical logic operation have been demonstrated in Refs.[1–3], such as the ultrafast nonlinear interferometer (UNI), interferometric wavelength converter (IWC), and several semiconductor optical amplifiers (SOAs), which can achieve all-optical logic operation.

Compared with these schemes, semiconductor optical amplifier loop mirror (SLALOM), also called terahertz optical asymmetric demultiplexer, has some advantages, such as powerful function, compact structure, signal amplification, wavelength flexibility, low control pulse energy, and large dynamic range. It has been proven to be one of the most promising all-optical logic operation mechanisms, and it has been exploited to achieve many logic operations,[4−7] such as all-optical full adder, all-optical parity checker, pseudorandom number generator, all-optical binary half-adder, and so on. Therefore, SLALOM would be a key functional element in all-optical signal processing.

In this paper, all-optical XOR and NOT logic operations are first demonstrated simultaneously based on SLALOM. At the same operation condition, the NOT logic operation could be achieved from the input port through a circulator, and the XOR logic operation could be achieved from the output port. In Section 2, a theoretical model and numerical calculation results are presented. In Section 3, experimental results for the two logic operations are discussed. Experimental results are in good agreement with calculated results.

2. Operation principle and numerical simulation

The schematic diagram of SLALOM is shown in Fig.1. The control pulse $P_{\rm in}(t)$ couples into the fibre loop mirror through the port C of coupler 2. A continuous wave, the power of which is much lower than that of control pulse so as to be unable to saturate

*Project supported by the State Key Development Programme for Basic Research of China (Grant No 2000036605) and the National High Technology Development Programme of China (Grant No 2002AA312160).

†E-mail: wangying_hust@yahoo.com.cn

SOA, couples into the fibre loop mirror through the port A of coupler 1, and splits into two counterpropagating signals: CW (clockwise) and CCW (counter-clockwise). The SOA is located asymmetrically in the fibre loop, and the offset distance from the mid-point of the fibre loop is Δx. The CCW light takes a time delay $2\Delta t = 2\Delta x/(n_{\text{eff}} \cdot c)$ later than the CW light ($2\Delta t < T$). Here T is the bit period of the input signal, and c is the velocity of light in vacuum.

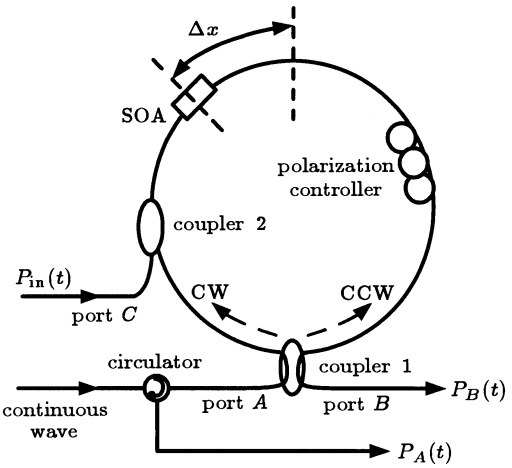


Fig.1. Schematic diagram of SLALOM. SOA: semiconductor optical amplifier; CW: clockwise; CCW: counter-clockwise

Having traversed the loop, the CW and CCW signal interfere at coupler 1. If the control pulse is logic '0', then CW and CCW signals have the same phase shift so that they interfere destructively at port B and interfere constructively at port A. Contrarily, if the control pulse is logic '1', the CW and CCW signals will experience different carrier density profile of SOA and have different phase shifts so that interference output appears at port B and port A simultaneously.

In SOA, the carrier rate equation and the wave-propagation equation could be written as [8]

$$\frac{\partial N}{\partial t} = \frac{J}{qd} - \frac{N(z,t)}{\tau} - \frac{\Gamma g P(z,t)}{h\nu A}, \tag{1}$$

$$\frac{\partial P(z,t)}{\partial z} = \Gamma g P(z,t) - \alpha_D P(z,t). \tag{2}$$

And g is the gain coefficient given by

$$g = g_N(N(z,t) - N_{\text{t}}) - r_2(\lambda - \lambda_{\text{p}})^2 + r_3(\lambda - \lambda_{\text{p}})^3. \tag{3}$$

Here N is the carrier density, N_{t} the transparency carrier density, τ the carrier lifetime, g_N the differential gain coefficient, P the optical power, h Planck's constant, ν the optical frequency, J the injection current density, q the electron charge, d the active layer thickness, α_D the internal loss coefficient of the active region, Γ the mode confinement factor, λ_{p} the peak wavelength, r_2 and r_3 are constants related to the gain bandwidth and gain asymmetry respectively, t is time and z is the propagation direction. Here, the amplified spontaneous emission is ignored since a SOA with a large signal input is concerned, and the facet residual reflectivity is also ignored for simplicity.

Usually SOA is divided into a number of thin longitudinal sections [9,10] in theoretical analysis. In this model all the sections are equal in length, and the carrier density within each section is assumed to be uniform. Then carrier density and power in each section is governed by the following equations:

$$\frac{\partial N_j}{\partial t} = \frac{J}{qd} - \frac{N_j(z,t)}{\tau} - \frac{\Gamma g_j P_j(z,t)}{h\nu A}, \tag{4}$$

$$\frac{\partial P_j(z,t)}{\partial z} = \Gamma g_j P_j(z,t) - \alpha_D P_j(z,t). \tag{5}$$

Here j represents the jth section in SOA. Then Eq.(6) can be derived from Eq.(5):

$$P_{j+1} = P_j \exp[(\Gamma g_j - \alpha_D)\Delta z]. \tag{6}$$

On the other hand, the induced phase shift is [11]

$$\Delta\phi = -\frac{\alpha}{2} \cdot \ln\left(\frac{G}{G_0}\right), \tag{7}$$

where

$$G_0 = \exp\left\{\Gamma g_N l\left(N_0 - N_{\text{t}} - \frac{r_2}{g_N}(\lambda - \lambda_{\text{p}})^2 + \frac{r_3}{g_N}(\lambda - \lambda_{\text{p}})^3\right) - \alpha_D \cdot l\right\}$$

is the small signal gain of SOA, $N_0 = \dfrac{J\tau}{qd}$, l is the length of SOA, α is the linewidth enhancement factor. So the output power of port B can be written as [12]

$$P_B(t) = P_{\text{in}}(t) \cdot \{s^4 G_{\text{CW}} + k^4 G_{\text{CCW}} - 2s^2k^2\sqrt{G_{\text{CW}} \cdot G_{\text{CCW}}} \cdot \cos(\Delta\phi)\}, \tag{8}$$

while the output power for port A is

$$P_A(t) = P_{\text{in}}(t) \cdot \{s^4 G_{\text{CW}} + k^4 G_{\text{CCW}} + 2s^2k^2\sqrt{G_{\text{CW}} \cdot G_{\text{CCW}}} \cdot \cos(\Delta\phi)\}. \tag{9}$$

Here, s and k represent the cross and through coupling ratios respectively. For an ideal 50:50 coupler, $s^2 = k^2 = 0.5$. $\Delta\Phi$ is the phase difference between CW and CCW signals at coupler 1, P_{in} is the input power of port C, G_{CW} and G_{CCW} represent the gain of CW and CCW signals respectively. All the parameters used in calculations are listed in Table 1.

Table 1. Parameters in numerical calculation.

Parameter	Value
length of the active layer l/μm	500
width of the active layer w/μm	2
depth of the active layer d/μm	0.1
mode confinement factor Γ	0.35
linewidth enhancement factor α	3.5
carrier lifetime τ/ps	100
differential gain coefficient g_N/m^2	6.3×10^{-20}
efficient index of active layer n_{eff}	3.5
internal linear loss of the SOA α_D/m^{-1}	4.0×10^{3}
carrier density at transparency $N_{\mathrm{t}}/\mathrm{m}^{-3}$	1.0×10^{23}
inject current I/mA	100
peak wavelength λ_{p}/m	1.55×10^{-6}

Because of the asymmetrical placement of SOA, it executes XOR operation of the CW signal and $2\Delta t$ delayed CCW signal at the port B,[13] and executes NOT operation of the input signal P_{in} at the port A.

The numerical simulation results are shown in Fig.2. The bit stream to port C labelled with $P_{\mathrm{in}}(t)$, which is shown in the upper figure of Fig.2(a), is 100011001110. The lower figure of Fig.2(a) indicates the logic NOT result of $P_{\mathrm{in}}(t)$. The CW signal and CCW signal shown in the upper figure of Fig.2(b) interfere to produce the XOR result that is shown in the lower figure of Fig.2(b).

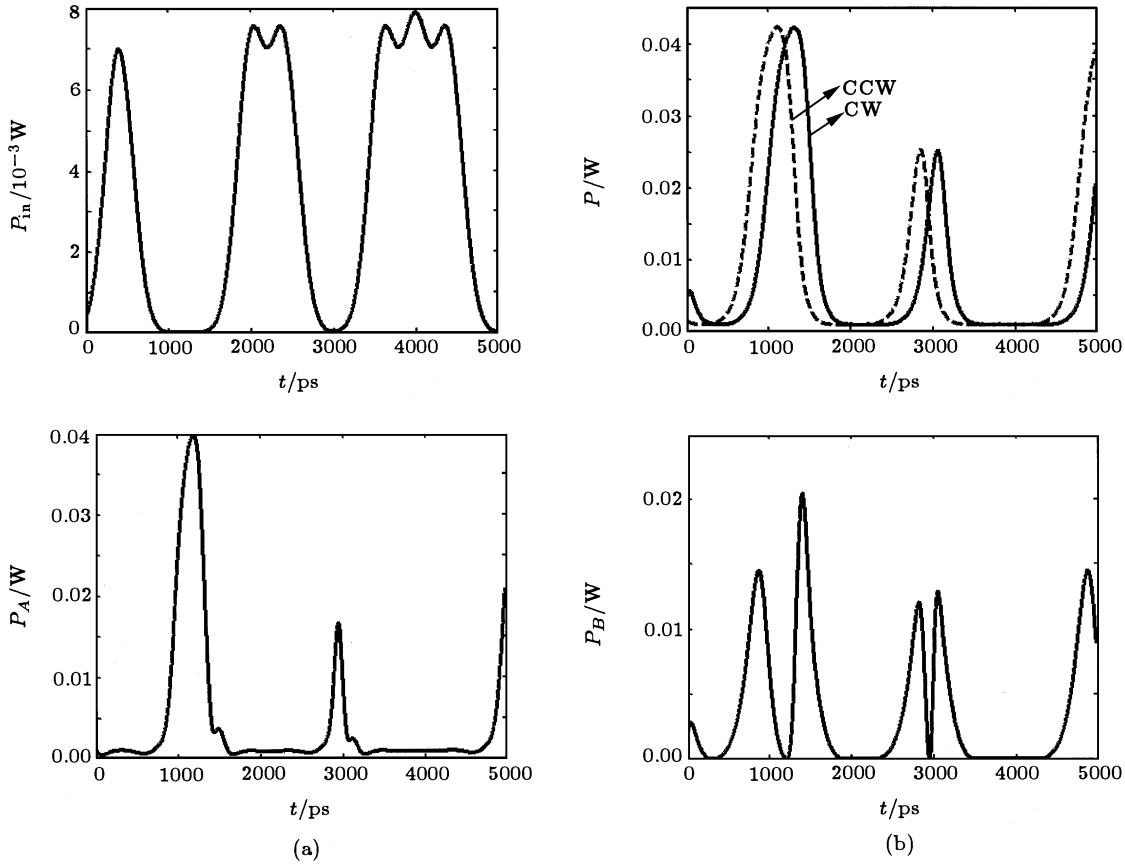


Fig.2. Numerical simulations for all-optical XOR and NOT operation processes. (a) The NOT operation result of input at port C; (b) the XOR operation result of CW signal and CCW signal.

3. Description of experiment and discussion of results

The experimental setup is shown in Fig.3. The travelling-wave SOA exploited in the experiment, which is based on tapered-cleaved active region with bulk material, is fabricated by OptoSpeed Co. Ltd. Its 3 dB saturation power is 5.9 dBm and its small signal gain is 18.9 dB. The two ends of the SOA are connected by the coupler 1 to construct a loop mirror, so port A and port B turn out to be the input and output ports of the SLALOM. A polarization controller is exploited to control the polarization state of CW and CCW signals to improve the output performance. In the experiment, $2\Delta t$ of the SLALOM is managed to set at 200 ps.

A SDH analyser, MP1570A of Anritsu Ltd, is used as signal source to generate bit streams (NRZ (non-return-zero) signal) at 1545 nm with 2.5 Gb/s to the port C. In order to saturate the SOA, these bit

streams should be amplified by EDFA and filtrated by bandpass filter before entering the SLALOM as shown in Fig.2. The continuous wave at 1554.5 nm obtained from a tunable laser enters the SLALOM from port A. After CW and CCW signals interfere at port A and port B, filter 2 (1554.5 nm) and filter 3 (1545 nm) are used to filtrate the output of port B and port A. Finally, a communication analyser, CSA8000 of Tektronix, is used to observe the output waveforms.

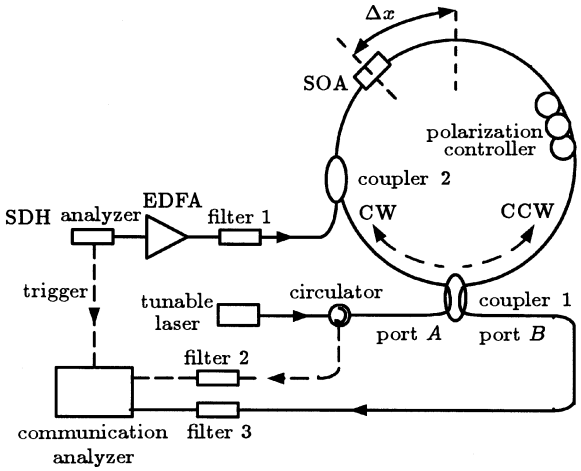


Fig.3. Experimental setup for all-optical XOR and NOT operations based on SLALOM. EDFA: erbium-doped fibre amplifier; SOA: semiconductor optical amplifier; SDH: synchronous digital hierarchy.

The input bit streams are shown in Fig.4(a). Then Figs.4(b) and (c) represent the outputs of the port B and port A respectively. Obviously they are in accordance with the results calculated in Section 2. In addition, this XOR operation function for CW and CCW signals executes a conversion from NRZ to PRZ (pseudo-return-zero), and this NOT operation for input bit streams executes a wavelength conversion. Therefore, the all-optical NOT and XOR operations are well realized.

As shown in Figs.4(a) and (b), compared with the input signals, the output pulse corresponding to the leading edge has a much higher amplitude than that corresponding to the trailing edge. The reason is that the leading edge of NRZ signals consumes so many carriers that the carrier density decreases rapidly, and thus the gain and phase of CW and CCW signals are quite different. Therefore the output pulse has a higher amplitude after the CW and CCW signals interfere with each other. In contrast, the carriers in SOA are slowly recovering at the trailing edge of the input signals so that the gain and phase of CW and CCW signals are slightly different.

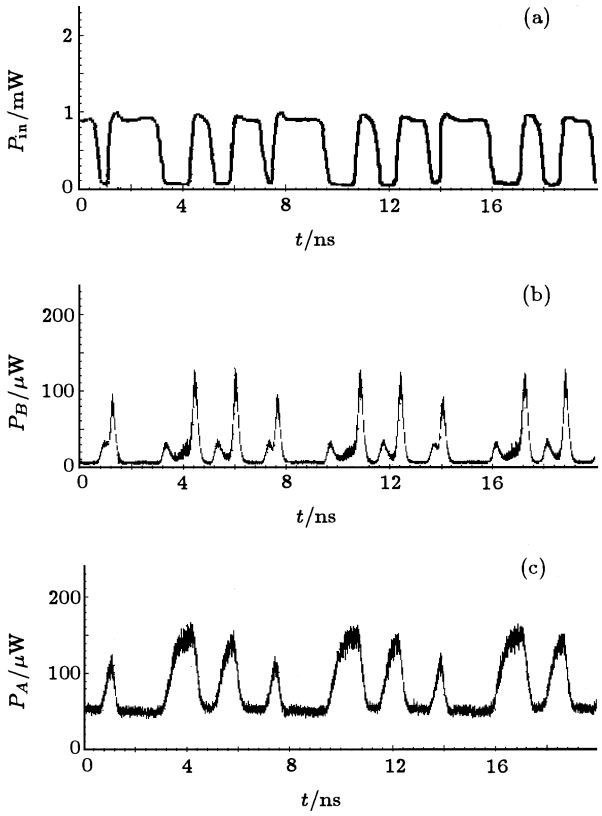


Fig.4. Experimental results for all-optical XOR and NOT operations. (a) The input signal of port C; (b) the output signal of port B; (c) the output signal of port A.

Compared with Fig.2(b), it can be seen in Fig.4(b) that the amplitude of the output pulse corresponding to the trailing edge of the input signal is much lower than that of the leading edge. The reason is that the carrier lifetime τ is set at 100 ps in our numerical simulation, and the practical carrier lifetime τ is about 400–1000 ps for a SOA of the bulk material. So the process of carriers recovering in the experiment is longer than that in theoretical simulation, and the output pulse corresponding to the trailing edge of the input signal has a lower gain.

The NOT operation result for the input bit streams shown in Fig.4(a) is illustrated in Fig.4(c). When the input signals emerge logic '1', the corresponding output of port A is logic '0'. When the input signals emerge logic '0', the corresponding output of port A is logic '1'. The output NOT operation result of input signals is also different in amplitude from bit to bit because of the pattern effect in the SOA.

It can be seen from Figs.4(b) and (c) that the output extinction-ratio of XOR operation is better than that of NOT operation. As the phase difference between the CW signal and CCW signal acquired in the SLALOM is generally $0 < \Delta\Phi < \pi$, when the input

signal is logic '1', $\Delta\Phi$ is too difficult to reach 'π' so as to hardly achieve destructive interference at port A.

4. Conclusion

In this paper, all-optical XOR and NOT operations based on SLALOM are demonstrated simultaneously at the same operation condition. Based on the segmented model of SOA, the all-optical logic operation process is simulated theoretically. In the experimental study, 2.5 Gb/s all-optical XOR and NOT logic operations are achieved based on SLALOM, the XOR operation was achieved in the output port, while the NOT operation was achieved in the input port through a circulator. The XOR operation function for the CW and CCW signals in loop mirror well executes a conversion from NRZ to PRZ, and the NOT operation executes an inverted wavelength conversion of the input signal. Owing to the limited carrier recovery time, there exists an obvious pattern effect in all-optical logic operations. Experimental results are in accordance with the theoretical simulation results.

References

[1] Bintjas C, Kalyvas M, Theophilopoulos G, Stathopoulos T, Avramopoulos H, Occhi L, Schares L, Guekos G, Hansmann S and Dall'Ara R 2000 *IEEE Photon. Technol. Lett.* **12** 824

[2] Fjelde T, Wolfson D, Kloch A, Dagens B, Coquelin A, Guillemot I, Gaborit F, Poingt F and Renaud M 2000 *Electron. Lett.* **36** 1863

[3] Kim J H, Jhon Y M, Byun Y T, Lee S, Woo D H and Kim S H 2002 *IEEE Photon. Technol. Lett.* **14** 1436

[4] Poustie A J, Blow K J, Kelly A E and Manning R J 1999 *Opt. Commun.* **168** 89

[5] Poustie A J, Blow K J, Kelly A E and Manning R J 1999 *Opt. Commun.* **162** 37

[6] Poustie A J, Blow K J, Manning R J and Kelly A E 1999 *Opt. Commun.* **159** 208

[7] Poustie A J, Blow K J, Kelly A E and Manning R J 1998 *Opt. Commun.* **156** 22

[8] Zhang X L, Sun J Q, Liu D M, Huang D X and Yi H Q 2000 *Acta Phys. Sin.* **49** 741 (in Chinese)

[9] Blow K J, Manning R J and Poustie A J 1998 *Opt. Commun.* **148** 31

[10] Zhang X L, Huang D X, Sun J Q and Liu D M 2001 *Chin. Phys.* **10** 124

[11] Zhang X L *Ph. D. Thesis* 2001 (Wuhan: Huazhong University of Science and Technology) (in Chinese)

[12] Eiselt M, Pieper W and Weber H G 1995 *J. Lightwave Technol.* **13** 2099

[13] Lee H J and Park C S 2000 *Opt. Commun.* **181** 323